Transient electrical and thermal responses of a 2-section BSCCO-2223 coil under overcurrent pulses

Akira Sugawara, Hisashi Isogami*, Karl W. Kowallis*, Yukikazu Iwasa*

Abstract— This paper presents experimental and numerical simulation results of a 2-section coil subjected to overcurrent pulses in the temperature range 20-60 K. The experiment simulates a high-temperature superconducting (HTS) magnet for electric devices such as fault-current limiters, transformers, motors, and power lines under fault-mode overcurrent pulses. Each section of the test coil is layer-wound with Bi-2223/Ag composite tape, 3.5-mm wide and 0.23-mm thick, with the outer section wound directly over the inner section. A pulse current exceeds the critical current of each conductor and may drive each section normal. A constant current that follows the pulse current leaves each section in three possible conditions: completely superconducting, recovering, and quenching. Simulation agrees reasonably well with experiment.

***Index Terms*— overcurrent pulse, HTS magnet, Bi-2223/Ag tape, quench/recovery, critical current.**

I. Introduction

Although it is generally agreed that HTS magnets are stable against most disturbances that afflict LTS magnets,[1] HTS magnets used in electric devices—fault-current limiters, motors, transformers, and power lines—require protection from fault-mode disturbances such as overcurrent pulses. If an overcurrent pulse exceeds the conductor's critical current for a long period of time, an incident that is likely to occur in the HTS magnet of a fault-current limiter, for example, the constant current that follows the pulse current leaves the HTS magnet in three possible conditions: completely superconducting, recovering, and quenching. This study focuses on an experimental and analytical study of the quench/recovery process of a test coil subjected to an overcurrent pulse.[2]

II. Experimental Setup

The test coil is composed of two concentric sections, inner and outer, connected in series and with the inner section wound over a copper coil form. Table I presents key parameters of each section.

Manuscript received September 17, 2000.

A. Sugawara is a visiting scientist (03/2000-03/2001) at MIT Francis Bitter Magnet Laboratory, Cambridge, MA 02139-4307, USA (e-mail: sugawara@jokaku.mit.edu). Permanent address: Dep. of Electrical and Electronic Eng., Niigata University, Japan (e-mail:akira@eng.niigata-u.ac.jp).

H. Isogami is a visiting scientist (03/2000-03/2001) at MIT Francis Bitter Magnet Laboratory, Cambridge, MA 02139-4307, USA (e-mail: isogami@jokaku.mit.edu). Permanent address: Mechanical Engineering Research Laboratory, Hitachi Ltd , Japan.

K. W. Kowallis was with MIT Francis Bitter Magnet Laboratory, Cambridge, MA 02139-4307, USA. Present address: 6251 Summer Pond Drive, Centerville, VA 20121-4644, USA (email: kowallis@npl.com).

Y. Iwasa is with MIT Francis Bitter Magnet Laboratory, Cambridge, MA 02139-4307, USA (telephone: 617-253-5548
e-mail: iwasa@jokaku.mit.edu).

TABLE I
TEST COIL PARAMETERS

	Inner Section	Outer Section
Inside Diameter[mm]	100.0	105.8
Outside Diameter[mm]	104.6	108.1
Wind Height[mm]	76.0	76.0
Total Turns	160	80
Layers	8	4
Turns/Layer	20	20
Conductor Length[m]	52	27.6
Self Inductance[mH]	2.37	1.43
Conductor Width[mm]	3.5	3.5
Conductor Thickness[mm]	0.23	0.23

A schematic drawing of the experimental setup is shown in Fig. 1.[3] The figure also includes a block diagram for the computer-based data acquisition system of the experiment. The principal experimental data are total voltages of, and pulse current through, both sections. The magnet temperature is measured with a diode sensor.

The test coil and a cryocooler are housed in a cryostat with its interior evacuated. The copper coil form of the test coil is attached and thermally anchored to the 2nd stage of a cryocooler. A heater attached to the 2nd stage controls the test coil operating temperature.

For a transport current of 100 **A**, the test coil generates a centerline field of 0.24 **T** and a peak field of 0.30 **T**. A large current pulse is applied for ～3 **s** and then the current decreases to a constant (nominal operating) current ～30 **A**. If the pulse current exceeds the critical current, the conductor is driven normal and a resistive voltage appears across the terminals of each section. Upon the application of an overcurrent pulse followed by a constant current, the test coil is left in one of the following three conditions: 1) superconducting; 2) quench/recovery; and 3) quench/nonrecovery.

A typical applied current waveform used in the experiment is shown in Fig. 2. The power supply is turned on at t = 0. After the overcurrent pulse length, typically 3 **s**, the current is reduced to a nominal operating level. After ～10 **s** at this constant level, the supply is shut off. Table II presents current waveform parameters of the corresponding response of the outer section for 6 runs; in each of these runs the inner section remained superconducting.[2] In the event of a quench/nonrecovery, the power supply was shut off within a few seconds after the end of the overcurrent pulse to keep the outer section from being overheated.

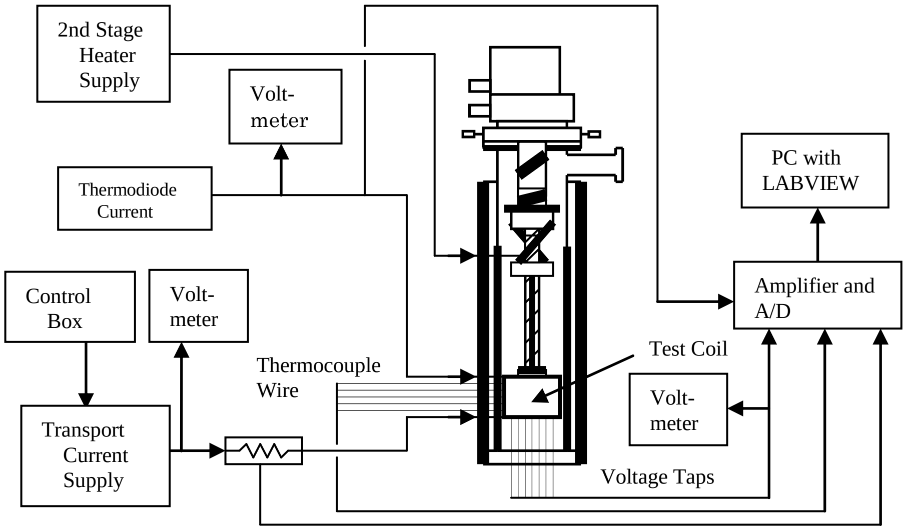

Fig. 1. Experimental setup.

III. Numerical Simulation

The thermal behavior of the conductor is governed by the following power density equation:

$$C_{cd}\frac{\partial T}{\partial t}=\nabla\cdot\left(k_{cd}\nabla T\right)+g\left(T,I_C\right)$$

T is conductor temperature, C_{cd} and k_{cd} are, respectively, the winding's volumetric heat capacity and thermal conductivity, both principally of silver and Kapton. C_{cd} and k_{cd} are strongly temperature dependent at cryogenic temperatures. $g(T,I_C)$ represents the Joule heating given by:

$$g\left(T,I_C\right)=\begin{cases} I_t\left(I_t-I_C\right)\dfrac{\rho_m}{x_m A} & \text{if } T<T_C \text{ and } I_t>I_C \\ I_t^2\dfrac{\rho_m}{x_m A} & \text{if } T\ge T_C \\ 0 & \text{if } T<T_C \text{ and } I_t\le I_C \end{cases}$$

I_t is a transport current; I_C is the conductor critical current; T_C is the conductor critical temperature; ρ_m is the matrix resistivity, which is a function of temperature and should be adjusted with a Kohler function for magnetic field; and $\chi_m A$ is the matrix metal cross-sectional area.

Figure 3 shows details of two adjacent layers. The conductor is barber-pole wrapped with 25-μm thick Kapton insulation, as depicted in the figure and further detailed in Fig. 4. The boundary condition assumes that heat flow from the test coil to the 2nd stage originates from the innermost layer of the inner section. For this particular study the entire magnet is driven normal by an overcurrent pulse, raising the magnet temperature uniformly over the entire winding of each section.

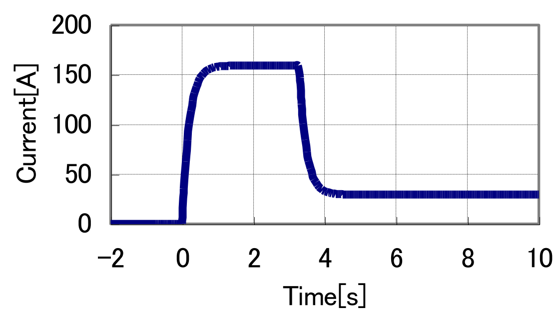

Fig. 2. An example of current waveform. A large pulse and operating current.

TABLE II
TRIAL DATA SUMMARY FOR OUTER SECTION

Run	Temperature [K]	Pulse Length [s]	Peak Curren t [A]	Operatin g Current [A]	Response
1	20	3.84	123.9	36.1	Superconducting
2	20	2.84	135.3	36.1	Quench/recovery
3	19	3.28	159.2	29.4	Quench/nonrecovery
4	39	3.06	120.2	27.6	Superconducting
5	39	2.94	128.2	27.6	Quench/recovery
6	39	3.00	130.6	27.7	Quench/nonrecovery

Numerical simulation uses a finite difference method. Each turn is divided into 8 elements with layers overlapping (Fig. 3). The conductor critical current data, $I_C(T)$, for each section are important inputs in the simulation. Figure 5 shows measured I_C data and $I_C(T)$ functions used in the simulation.

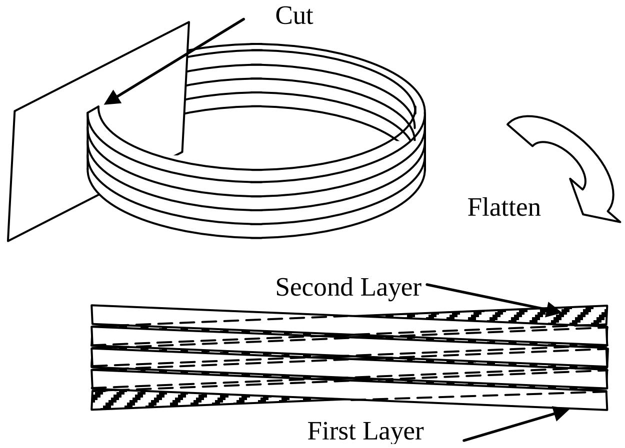

Fig. 3. Detail of two adjacent layers

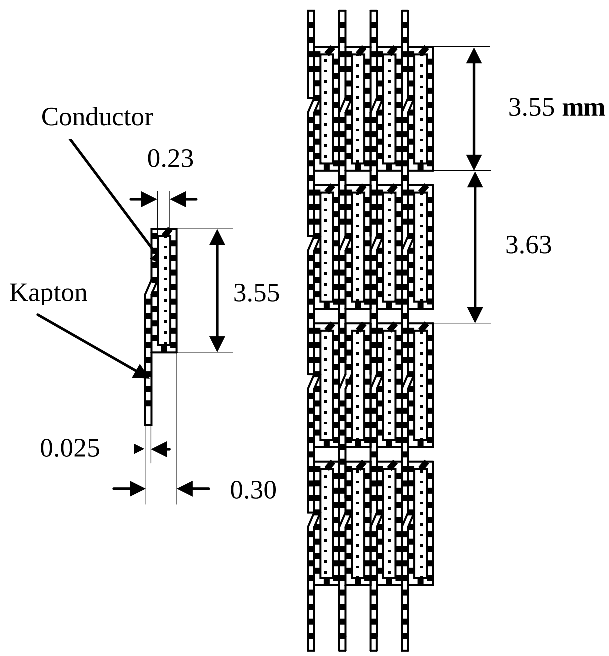

Fig. 4. Details showing conductor and insulator.

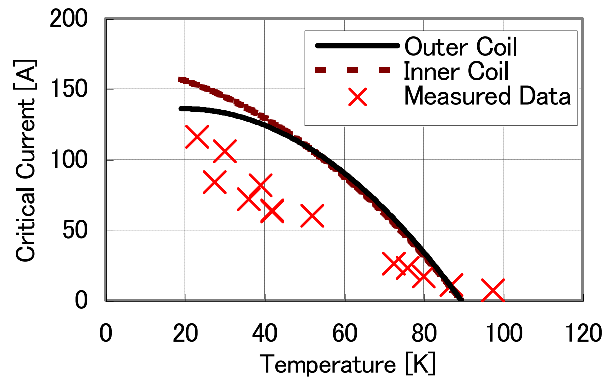

Fig. 5. Critical current curves estimated for the simulation and measured data (X).

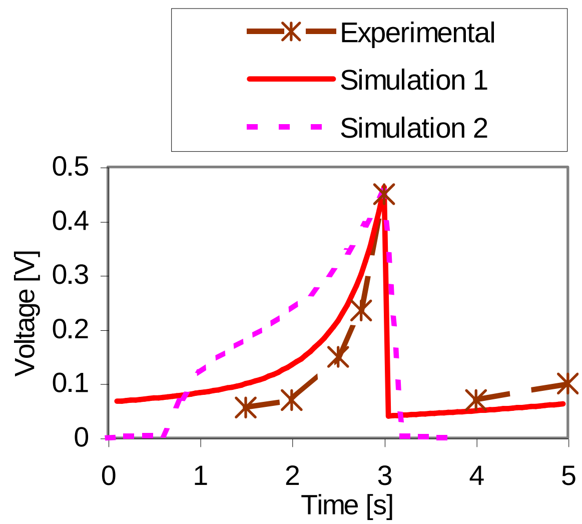

Fig. 6. An example of experimental result and numerical simulation from Run 6. Simulation 1: The magnetic flux density is spatially variable. Simulation 2: The magnetic flux density is uniformly 0.3 **T**.

IV. Results and Discussions

Figure 6 shows three $V(t)$ traces of the outer section from Run 6 (Table II), one experimental[3] and the other two simulations (Simulation 1 and Simulation 2); the inner section remained superconducting. The coil current is 130.6 **A** for $0 \leqq t \leqq 3.0$ **s** and 27.7 **A** for $t \geqq 3.0$ **s**. During the overcurrent pulse, the resistive voltage increases with time; a sharp increase near the end of the pulse indicates a full-scale quench would ensue if the current was kept at 130.6 **A**. Simulation 1 (solid) agrees with the experimental trace better than Simulation 2 (dashed). The only difference between two simulation codes is spatial field distribution within the coil winding: Simulation 1 code includes the spatial variation, while Simulation 2 assumes it constant.

Figure 7 shows a spatial field distribution over the coil cross section at 100 **A**. Within the outer section, the total field increases axially away from the midplane, due entirely to the increase in B_r. This spatial variation in field creates a spatial variation in I_C, which in turn generates spatially varying Joule dissipation within the outer section, a result of which is a time-varying spatial temperature distribution within the outer section winding. Figure 8 shows a temperature distribution within the coil winding at t=3.0 **s** for Run 6, computed with simulation code. Note that except at and near each end of the outer section where the temperature is at or close to a maximum level of 65 **K**, the rest remains close to the operating temperature of 39 **K**. Despite being exposed to, on average, a field level much higher than that in the outer section, reasons that the inner section could remain superconducting are its: 1) better thermal coupling to the copper coil form; and 2) slightly higher $I_C(T)$.

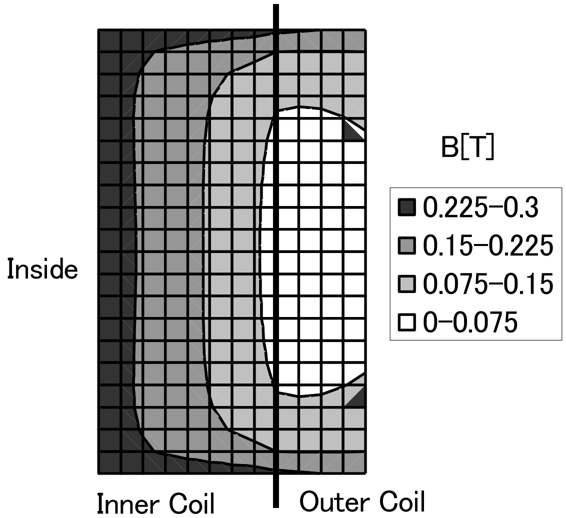

Fig. 7. Magnetic flux density distribution at 100 **A**.

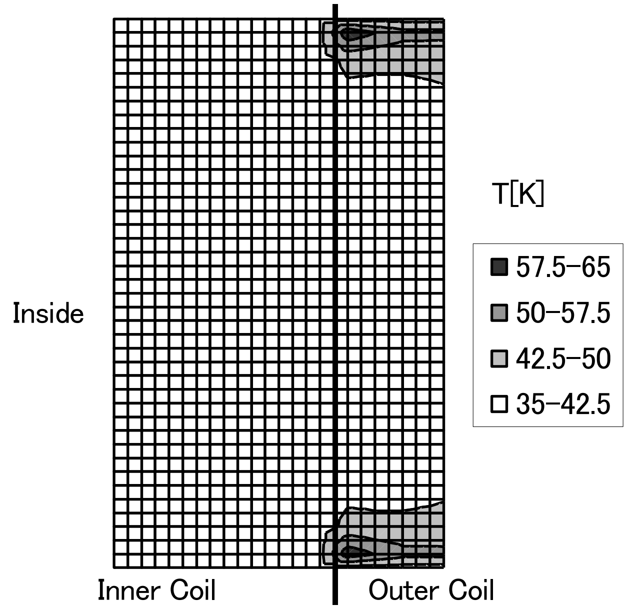

Fig. 8. Temperature Distribution at *t*=3.0 **s** in Run 6.

V. CONCLUSIONS

A 2-section test coil, each section layer-wound with Bi-2223/Ag, was studied experimentally and analytically for its quench/recovery behaviors in the operating temperature range 19-39 **K**. For a given overcurrent pulse followed by a constant current, the test coil responds in one of the following ways: 1) remains superconducting; 2) quenches but recovers; or 3) quenches and does not recover. For 6 experimental runs, although the inner section always remained superconducting, the outer section showed all three responses.

REFERENCES

[1] Y. Iwasa, "*Case Studies in Superconducting Magnets*," Chapter 6 and Appendix Ⅲ, Plenum Press, New York, 1994..

[2] Y. Iwasa, "Protection for HTS windings," *Presentation at the DOE Annual Peer Review Meeting on Superconductivity Programs for Electric Power Systems* (July 19, 1999, Washington DC).

[3] Karl W. Kowallis, "Transient thermal recovery of a pulsed BSCCO-2223 superconducting magnet," *S.M. Thesis* (Department of Mechanical Engineering, MIT, 2000).